Shape-Dependent Oriented Trapping and Scaffolding of Plasmonic Nanoparticles by Topological Defects for Self-Assembly of Colloidal Dimers in Liquid Crystals

Bohdan Senyuk,[†] Julian S. Evans,[†,‡] Paul J. Ackerman,[†] Taewoo Lee,[†] Pramit Manna,[§] Leonid Vigderman,[§] Eugene R. Zubarev,[§] Jao van de Lagemaat,[‡,□] and Ivan I. Smalyukh*[,†,□]

[†]Department of Physics, Materials Science and Engineering Program, Department of Electrical, Computer, and Energy Engineering, and Liquid Crystals Materials Research Center, University of Colorado at Boulder, Boulder, Colorado 80309, United States

[‡]National Renewable Energy Laboratory, Golden, Colorado 80401, United States

[§]Department of Chemistry, Rice University, Houston, Texas 77005, United States

[□]Renewable and Sustainable Energy Institute, National Renewable Energy Laboratory and University of Colorado at Boulder, Boulder, Colorado 80309, United States

ABSTRACT: We demonstrate scaffolding of plasmonic nanoparticles by topological defects induced by colloidal microspheres to match their surface boundary conditions with a uniform far-field alignment in a liquid crystal host. Displacing energetically costly liquid crystal regions of reduced order, anisotropic nanoparticles with concave or convex shapes not only stably localize in defects but also self-orient with respect to the microsphere surface. Using laser tweezers, we manipulate the ensuing nanoparticle-microsphere colloidal dimers, probing the strength of elastic binding and demonstrating self-assembly of hierarchical colloidal superstructures such as chains and arrays.

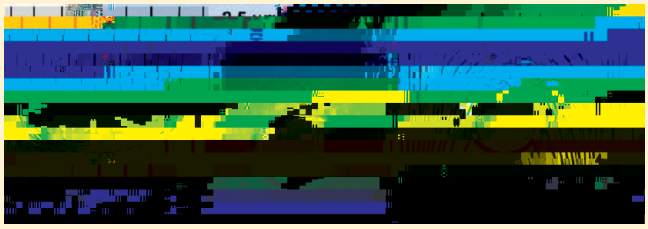

KEYWORDS:

attracted to defects to displace the energetically costly defect

dimethylammonium chloride (DMOAP) to set vertical surface boundary conditions for the LC molecular alignment.[25] Melamine resin spherical particles of 2 μm in diameter and with tangential surface boundary conditions[26] were obtained in an aqueous dispersion (from Sigma-Aldrich) and turned into a powder via slow water drying. These microparticles were then dispersed in the LC by direct mixing and a 15−30 min sonication to break apart pre-existing colloidal aggregates. Gold nanoparticles were dispersed from ethanol to toluene and then added to the mixture of LC and microspheres; toluene was evaporated afterward. This colloidal dispersion was sonicated for 30−60 min while slowly changing the samples' temperature from isotropic to the LC state to obtain isolated microspheres and metal nanoparticles in the nematic host. Using capillary forces, LC colloidal dispersions were filled into ∼5−10 μm thick cells formed by substrates spaced by glass fiber spacers and treated to provide planar or vertical boundary conditions. In order to set homogeneous planar boundary conditions, glass plates were spin-coated with polyimide PI2555 (HD Micro-System) on their inner surfaces, unidirectionally rubbed, and then glued together by epoxy while aligned to have "antiparallel" rubbing directions at the opposite plates. Surface treatment of substrates with DMOAP was used to set the vertical surface boundary conditions for the LC molecules.

We have used dark-field, bright-field, and polarizing modes of optical imaging with an inverted Olympus microscope IX81 integrated with a holographic optical trapping (HOT) setup[27] operating at wavelength λ = 1064 nm. The strong scattering of metal nanoparticles[28] in the dark-field microscopy

as the dark-field and polarizing microscopy images shown in Figure 1f for the case of SFs shown in Figure 1b. MG nanoparticles (Figure 1a) have the shape of a pentagonal prism and align in the nematic LC with their long dimension L_{np} normal to $\mathbf{n_0}$ (Figure 1j). Because of the homeotropic surface anchoring, they are encircled by a disclination loop of strength $k = -1/2$ (Figure 1j), where k is defined as a number of director turns by 2π when the defect core is circumnavigated once. MGs freely rotate around $\mathbf{n_0}$. NB nanoplatelets (Figure 1c) with multiple irregular sharp edges and vertical surface boundary conditions align with their flat sides normal to $\mathbf{n_0}$, inducing a $k = -1/2$ disclination loop around their perimeter (Figure 1l). The SFs have complex elongated shape with the concave base in the form of a star (Figure 1b). They align with their long axes along $\mathbf{n_0}$ and, as can be seen from polarizing microscopy textures (inset of Figure 1f), induce $\mathbf{n(r)}$ of quadrupolar symmetry with two surface point defects called "boojums" at their ends (Figure 1k). This $\mathbf{n(r)}$ structure can be explained by the grooved surface relief of the rodlike SF nanoparticles with star-shaped base (Figure 1b). Bulk elastic energy is minimized when the LC director locally follows these grooves instead of satisfying antagonistic surface boundary conditions exerted by the complex ribbed surface relief of these nanoparticles (Figure 1f,k), explaining the observed $\mathbf{n(r)}$-configuration. GNR and sGNR particles have octagonal cross sections. GNRs promote vertical alignment of LC molecules at their surface and align with their long axes along $\mathbf{n_0}$ with the $k = -1/2$ disclination loop encircling them in the plane normal to their long axis (Figure 1m). Since is small, one can expect that this disclination loop is "virtual" or located at the particle surface.[32−34] The anchoring at sGNR polystyrene-capped surfaces is tangential, causing weak $\mathbf{n(r)}$-distortions of quadrupolar symmetry with two boojums (Figure 1n). These findings for complex-shaped colloids are consistent with the studies of colloidal cylinders in LCs,[32,33,35−37] which showed that their orientation can be both along and perpendicular to $\mathbf{n_0}$ for normal boundary conditions and that rods with tangential boundary conditions typically align parallel to $\mathbf{n_0}$.

To enable and control spatial localization of fluid-borne nanoparticles of varying sizes and shapes, we use colloidal microspheres also dispersed in the LC. These solid microspheres induce much stronger distortions of $\mathbf{n(r)}$ compared to the nanoparticles, causing well-defined singular point and line

isotropic defect cores by the nanoparticles. We have used the HOT system[27] to translate the microspheres to the vicinity of metal nanoparticles. Dark-field video microscopy then tracked the motion of colloids after releasing the microparticles in the vicinity of nanoparticles. The sGNRs, GNRs (Figure 3a,i), and NBs (Figure 4a) were attracted toward point and line defects within a couple micrometers and eventually trapped by them (Figures 3a,c,e,g,h and 4a–c). Figures 3a and 4a show such nanoparticles being attracted into the point defect in the direction roughly along $\mathbf{n}_0$. The entrapment of nanorods by the Saturn ring defect around microsphere is demonstrated in Figure 3i,j. At large distances, the directionality of the elastic interactions between the microsphere and GNR is similar to that of two quadrupolar LC colloids with Saturn rings and the same curvature of $\mathbf{n}(\mathbf{r})$-distortions,[38,39,42] repelling at center-to-center separation vectors parallel and perpendicular to $\mathbf{n}_0$ but attracting at intermediate angles (Supporting Information Figure S4).[38,39,42] Even when released with center-to-center vector orientation corresponding to repulsion (Figure 3j), the GNR slowly drifts to the attractive angular sector and attracts toward the microsphere roughly along the expected direction of maximum attraction between such quadrupoles.[38,39,42] Once in the vicinity of the microsphere, the GNR slides around its surface by continuously displacing increasingly stronger director distortions and eventually localizes in the defect (Figure 3j). In contrast, the directionality of the elastic interactions between microsphere with the Saturn ring and sGNR with two boojums (Figure 3j) is similar to the case of two quadrupolar LC colloids having opposite distributions of defect signs and opposite curvature of $\mathbf{n}(\mathbf{r})$-distortions,[43] attracting at center-to-center separation vectors parallel and perpendicular to $\mathbf{n}_0$ but repelling at the intermediate angles (Supporting Information Figure S4). When released having the center-to-center separation vector perpendicular to $\mathbf{n}_0$, sGNRs head straight to the disclination until entrapped (Figure 3j). Once trapped in the point defect, sGNRs and GNRs spontaneously orient orthogonally to the sphere surface and along $\mathbf{n}_0$, as revealed by polarized TPL. GNRs and sGNRs trapped in disclinations align along the defect lines, minimizing the total free energy by maximizing the volume of melted defect core that they displace at this orientation.

Figure 4 shows that NB nanoplatelets are attracted to the point defect not only from close proximity (Figure 4a) but even when released at distant initial locations on the side of the microsphere opposite to that of the defect, moving down the path corresponding to the strongest gradient of $\mathbf{n}(\mathbf{r})$ (Figure 4e). Defect-trapped NBs orient to have their large-area faces locally parallel to the surface of the microsphere (Figure 4b,c and Supporting Information Figure S3). Several NBs can be collected in the region of the point defect simultaneously while preserving this orientation with respect to the microsphere (Figure 4e).

By tracking positions of colloids with video microscopy

distance and orientation with respect to the surface of the microsphere. The distance from the center of microsphere to the hyperbolic point defect is known to be $\sim$1.2a,[38,39] where a is the radius of the microsphere, while the radius of the Saturn ring defect is typically $\sim$1.1a.[41] By controlling the size of the colloidal microspheres in the submicrometer and micrometer ranges as well as controlling the size and shape of entrapped nanoparticles, one can use the demonstrated scaffolding of nanoparticles to form two-particle nanoantennas with the distance between the surfaces of bigger and smaller colloids controlled within 10−100 nm. One can also envision the assembly of ring-shaped structures of multiple plasmonic nanoparticles entrapped and oriented in the Saturn ring defect line encircling a bigger metallic or dielectric colloidal sphere. In addition to microspheres, one can utilize bigger particles of other shapes, like platelets and rings that are known to induce different types of defects.[44] Importantly, all of these fluid-borne colloidal microparticles with scaffolded nanoparticles can be further used for self-assembly or light-guided hierarchical superstructures with a host of potential applications, such as fabrication of novel types of tunable metamaterials.

In conclusion, we have demonstrated oriented trapping of plasmonic gold nanoparticles by topological singularities in nematic LCs. The defect traps induced by colloidal microspheres allow for highly precise, oriented spatial localization, strong maximum trapping potentials of 100−5000 k_BT, and large trap stiffnesses that depend on the shape and size of trapped nanocolloids and are of great interest for fundamental studies in nanophotonics and plasmonics. The demonstrated elastic scaffolding of smaller nanoparticles by elastic distortions and defects due to bigger microparticles yields an interesting colloidal system with the anisotropic nanoparticles at well-defined orientation with respect to the surface of microparticles and the far-field LC director. The ensuing colloidal dimers of plasmonic metal nanoparticles and dielectric microparticles can be assembled into a number of one- and two-dimensional arrays of desired configuration, as needed for applications in nanoscale photonics and plasmonics. The use of metal microparticles instead of dielectric ones may enable applications in nanoantennas as well as in nanoscale energy conversion systems. Similar approaches may be used for nanoscale trapping of other types of nanoparticles, like semiconductor nanocrystals, which are important for imaging and energy conversion. Since self-assembled structures of plasmonic nanoparticles can exhibit a broad range of magnetic and electric resonances,[7] plasmonic nanoparticle self-assemblies in a fluid LC medium with facile response to electric fields may offer a means for low-voltage control of their optical response and enable self-assembly based fabrication of tunable bulk metamaterials.

■ ASSOCIATED CONTENT

Ⓢ Supporting Information

Additional details regarding the two-photon luminescence from used gold nanorods and elastic interactions between quadrupolar colloids and movies showing the attraction of gold nanoparticles into topological singularities. This material is available free of charge via the Internet at http://pubs.acs.org.

■ AUTHOR INFORMATION

Corresponding Author

*E-mail: ivan.smalyukh@colorado.edu.

■ ACKNOWLEDGMENTS

This work was supported by the Division of Chemical Sciences, Geosciences, and Biosciences, Office of Basic Energy Sciences of the U.S. Department of Energy under Contract No. DE-AC36-08GO28308 with the National Renewable Energy Laboratory (J.vdL and J.S.E.), by the International Institute for Complex Adaptive Matter (B.S.), and by NSF Grants DMR-0847782, DMR-0820579, and DMR-0844115 (I.I.S., B.S., P.J.A., and T.L.). E.R.Z. acknowledges financial support by NSF (DMR-0547399, DMR-1105878). We thank Christian Schoen and Shelley Coldiron from Nanopartz, Inc. for providing gold nanoparticles along with the corresponding TEM images (Figure 1a,c,d). We acknowledge discussions with Nick Abbott, Noel Clark, and Victor Pergamenshchik.

■ REFERENCES

(1) Lal, S.; Link, S.; Halas, N. J. Nat. Photonics **2007**, 1, 641−648.
(2) Jain, P. K.; Huang, X.; El-Sayed, I. H.; El-Sayed, M. A. Acc. Chem. Res. **2008**, 41, 1578−1586.
(3) Sau, T. K.; Rogach, A. L.; Jäckel, F.; Klar, T. A.; Feldmann, J. Adv. Mater. **2010**, 22, 1805−1825.
(4) Morfa, A. J.; Rowlen, K. L.; Reilly, T. H.; Romero, M. J.; van de Lagemaat, J. Appl. Phys. Lett. **2008**, 92, 013504.
(5) Perassi, E. M.; Hernandez-Garrido, J. C.; Sergio Moreno, M.; Encina, E. R.; Coronado, E. A.; Midgley, P. A. Nano Lett. **2010**, 10, 2097−2104.
(6) Habteyes, T.; Dhuey, S.; Cabrini, S.; Schuck, P. J.; Leone, S. R. Nano Lett. **2011**, 11, 1819−1825.
(7) Fan, J. A.; Wu, Ch.; Bao, K.; Bao, J.; Bardhan, R.; Halas, N. J.; Manoharan, V. N.; Nordlander, P.; Shvets, G.; Capasso, F. Science **2010**, 328, 1135−1138.
(8) Shalaev, V. M. Nat. Photonics **2007**, 1, 41−48.
(9) Romero, M. J.; van de Lagemaat, J. Phys. Rev. B **2009**, 80, 115432.
(10) Ni, W.; Ambjörnsson, T.; Apell, S. P.; Chen, H.; Wang, J. Nano Lett. **2010**, 10, 77−84.
(11) Johnson, J. C.; Reilly, T. H.; Kanarr, A. C.; van de Lagemaat, J. J. Phys. Chem. C **2009**, 113, 6871−6877.
(12) Khatua, S.; Chang, W.-S.; Swanglap, P.; Olson, J.; Link, S. Nano Lett. **2011**, 11, 3797−3802.
(13) Dorfmüller, J.; Dregely, D.; Esslinger, M.; Khunsin, W.; Vogelgesang, R.; Kern, K.; Giessen, H. Nano Lett. **2011**, 11, 2819−2824.
(14) Alvarez-Puebla, R. A.; Agarwal, A.; Manna, P.; Khanal, B. P.; Aldeanueva-Potel, P.; Carbo-Argibay, E.; Pazos-Perez, N.; Vigderman, L.; Zubarev, E. R.; Kotov, N. A.; Liz-Marzan, L. M. Proc. Natl. Acad. Sci. U.S.A. **2011**, 108, 8157−8161.

(25) Koenig, G. M.; Lin, I.-H.; Abbott, N. L. Proc. Natl. Acad. Sci. U.S.A. **2010**, 107, 3998−4003.
(26) Smalyukh, I. I.; Kachynski, A. V.; Kuzmin, A. N.; Prasad, P. N. Proc. Natl. Acad. Sci. U.S.A. **2006**, 103, 18048−18053.
(27) Trivedi, R. P.; Engström, D.; Smalyukh, I. I. J. Opt. **2011**, 13, 044001.
(28) van de Hulst, H. C. Light Scattering by Small Particles, 2nd ed.; Dover Publications, Inc.: New York, 1981.
(29) Koenig, G. M.; de Pablo, J. J.; Abbott, N. L. Langmuir **2009**, 25, 13318−13321.

Supporting Information

Shape-dependent oriented trapping and scaffolding of plasmonic nanoparticles by topological defects for self-assembly of colloidal dimers in liquid crystals

Bohdan Senyuk,[†] Julian S. Evans,[†,‡] Paul J. Acker8 Tf ..998092 0 Eae[illegible]

A tunable (680-1080 nm) femtosecond Ti:sapphire oscillator (140 fs, 80 MHz, Chameleon Ultra-II, Coherent) was used to generate TPL from sGNRs. The

S2). The TPL from nanorods is excitation polarization dependent.[S1,S2] Figure S2 shows TPL images taken for two orthogonal polarizations of excitation beam. The brightest spots correspond to nanorods aligned parallel to the polarization of excitation beam and, from a superimposed image (Fig. S2c), one can distinguish the orthogonally oriented nanorods.

Figure S2. TPL images of nanorods sGNR spin-coated on glass cover slip taken at two orthogonal polarizations of excitation beam: (a) TPL image at vertical polarization; (b) TPL image at horizontal polarization; (c) superimposed image of (a) and (b). White double arrow shows the polarization of excitation beam. Excitation wavelength was 850 nm.

It is relatively difficult to determine the orientation of NB platelets at the surface of microsphere using the polarized dark-field microscopy as the scattering from microsphere usually overshadows the scattering from NB. Therefore, we also use TPL imaging with excitation at 850 nm to verify the orientation of NB nanoparticles nearby the microsphere surface (Fig. S3). The plasmonic response of NB is rather complicated due to the complex irregular shape of their edges. Nevertheless, the intensity of emission from NB is strongly dependent on the polarization of the excitation beam (Fig. S3). The emission intensity is maximum for the laser excitation with linear polarization perpendicular to the director (parallel to the flat surface of NB) (Fig. S3a) and minimum when the polarization of excitation is parallel to the director (perpendicular to the flat surface of NB) (Fig. S3b). This, along with the consideration of the known surface boundary conditions for the LC director, allowed us to conclude that the flat surfaces of NB nanoparticles orientate parallel to the surface of colloidal microsphere.

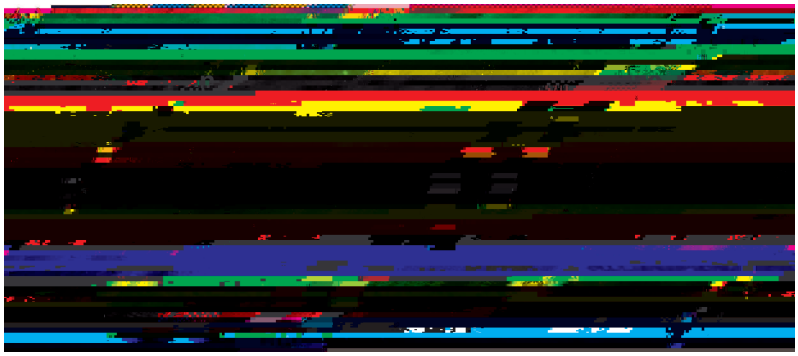

Figure S3. TPL images of the NB nanoparticle elastically entr